Structures 54 (2023) 106–116

Contents lists available at ScienceDirect

Structures

journal homepage: www.elsevier.com/locate/structures

Reliability analysis of controlled structures based on probabilistic active controller

Azadeh Jalali, Hashem Shariatmadar *

Department of Civil Engineering, Faculty of Engineering, Ferdowsi University of Mashhad, Mashhad, Iran

ARTICLE INFO

Keywords:
Reliability analysis
Monte Carlo method
Probabilistic fuzzy logic controller
Linear quadratic regulator

ABSTRACT

The reliability of controlled structures has been a subject of considerable concern in recent years. The present study investigated the effects of a probabilistic fuzzy logic controller (PFLC) as an intelligent controller and a linear quadratic regulator (LQR) controller as a classic controller on the reliability of a structure. Monte Carlo reliability analysis has been used to determine the reliability of the controlled structures. A single-degree-of-freedom (SDOF) system and multiple-degree-of-freedom (MDOF) structures with different tendon arrangements were considered. The structures were subjected to random Gaussian white noise as excitation and the variables considered were random Gaussian samples with a dispersion coefficient of 10%. The probability of failure could be estimated by PFLC at up to 10^{-5} as the threshold level increased in MDOF structures. Moreover, the results indicate that PFLC was more accurate than the LQR controller for a lower probability of failure because the associated limit state function includes stochastic uncertainty.

1. Introduction

The concept of reliability and safety in the structural control of civil engineering structures has been of major concern in recent decades. Different control systems have been proposed in consideration of the uncertainties and complexities present in engineering structures. Performance loss and instability and even structural failure indicate the occurrence of extreme vibration as a result of unforeseen structural control criteria.

Uncertainties and complexities can result from different sources and through the lack of information. The features of uncertainty differ and include linguistic (non-stochastic) uncertainty and stochastic uncertainty. Conventional fuzzy logic is a mechanism through which linguistic complexity can be managed and controlled. This requires the application of expert knowledge in the form of rules for unknown membership functions (MFs). However, the information available about the creation of fuzzy rules also contains non-stochastic uncertainty. To better consider uncertainty, a type-2 fuzzy logic system and interval type-2 fuzzy logic systems have been developed [1–10]; however, stochastic uncertainty has not been considered in fuzzy logic systems. Stochastic uncertainty is described by possibility and a random probability distribution.

A fuzzy logic system (FLS) with probabilistic features must be employed to process uncertainties which include both fuzzy and likelihood aspects. A probabilistic fuzzy logic system (PFLS) was introduced by Meghdadi and Akbarzadeh [11] which utilizes a three-dimensional (3-D) MF model to demonstrate stochastic uncertainty. A probabilistic MF requires 3-D information comprising one dimension for the input signal, one for the fuzzy grade in [0, 1] and one for the associated likelihood. The third dimension can be used to evaluate and express stochastic uncertainties using a probability distribution function (PDF).

Li et al. [12] and Liu et al. [13] proposed a simple tutorial for modeling and learning PFLS when both fuzzy and stochastic uncertainties occur. Zhang and Li [14] introduced a unified probabilistic fuzzy inference method to improve PFLS performance. Further, Zhang et al. [15] proposed a reasonable model of wind speed estimation using probabilistic fuzzy theory.

As the complexities and uncertainties of civil engineering structures increase and there is great need for controlling their effects, a probabilistic fuzzy logic controller (PFLC), as a probabilistic active control strategy, could be applicable. A PFLC can be used to better consider both linguistic and stochastic uncertainties, as uncertainty can cause a decrease in efficiency and increase the probability of failure. Studies have demonstrated that the reliability and safety of buildings can be improved by adding active control to structural engineering systems.

Spencer et al. [16] introduced a reliability-based optimal control

* Corresponding author.
E-mail addresses: azadeh.jalali@mail.um.ac.ir (A. Jalali), shariatmadar@um.ac.ir (H. Shariatmadar).

https://doi.org/10.1016/j.istruc.2023.05.039
Received 31 December 2022; Received in revised form 6 April 2023; Accepted 9 May 2023
Available online 19 May 2023

approach for a seismically excited single-story structure with parametric uncertainty. Their research focused on increasing the safety and reliability of a structure by minimizing its intense response. They used probabilities, the first-order reliability method second-order reliability method and Monte Carlo (MC) simulation. Spencer et al. [17] investigated the Kalman filter, linear quadratic regulator (LQR) and phase-corrected controllers to assess the reliability of SDOF structures. The Kalman filter and acceleration feedback controllers were considered for a three-story building.

Battani et al. [18] proposed an approach to use a control mechanism in reliability evaluation of a structural system. A three-story building with an active mass damper actuator on the third floor was considered. The structural responses considered were the acceleration of each floor, ground acceleration and actuator displacement. Sensitivity analysis was performed in the global reliability assessment. May and Beck [19] used an active mass driver benchmark system where controllers were proposed to reduce the failure probability of closed-loop procedures. To approximate the probability integrals, an asymptotic approach was applied to determine the efficiency of the process.

Venini and Mariani [20] proposed a state-space structure on which to conduct reliability analysis of unpredictable structures using an active controller and probabilistic excitation. In both the controlled and uncontrolled states, the reliability was measured using asymptotic techniques that did not require conversion to normal variations. For control synthesis, linear quadratic Gaussian (LQG) and H-infinity (H_∞) approaches were used to obtain the statistics of the managed device.

Field and Bergman [21] established a relationship between a desirable degree of reliability for a given system and configuration of the state covariance that allowed this level of reliability. The resulting configuration of the state covariance controller ensured that the specified reliability level was possible for a closed-loop system. This method was extended to single-story and two-story structures. Shariatmadar and Behnam [22] proposed a subset simulation method to compute small failure probabilities for controlled structures.

A non-probabilistic time-dependent reliability approach combined with active control theory was introduced by Wang et al. [23] to investigate the reliability of controlled buildings. The uncertain structural responses were analyzed by a closed-loop control. An integral non-probabilistic time-dependent reliability evaluation then was carried out for the active control procedure. In functional implementation, because of the of inadequate sample data, the distributions of some parameters may not be precisely understood. To overcome this problem, Zhang et al. [24] suggested a likelihood-unreliability hybrid approach to determine the reliability index and structural reliability according to chance theory, which can be applied to solve the problem of integrating likelihood and unreliability theories.

In consideration of uncertainties from various sources, Wang et al. [25] proposed a novel two-stage dimension-reduced dynamic reliability evaluation method for improving the efficiency of LQR-controlled structures. To simplify the system uncertainty process, non-probabilistic approaches to quantifying uncertainty were proposed by Wang et al. [26]. A controller that has been designed using a deterministic system may fail when applied to a real system because the parameters remain undetermined in real engineering. To solve this problem, Liu and Wang [27] proposed the methods of uncertain vibration active control systems with non-probabilistic time-dependent reliability and artificial neutral networks.

To the best of the authors' knowledge, no study has been focused on reliability analysis of probabilistic active controlled structures in which a PFLC has been applied to civil engineering structures. The PFLC is a combination of fuzzy and stochastic theories. The present study investigated the effects of two structural control systems on the reliability analysis of engineering structures with uncertain specifications that have been subjected to a dynamic random load which has been formulated using Gaussian white noise. One of the control strategies uses an intelligent PFLC as a probabilistic active controller and the other uses a classic LQR controller.

Monte Carlo reliability analysis has been used to estimate the reliability of controlled buildings. The dynamic parameters of structures such as the mass, stiffness and damping variables have been considered as random Gaussian variables with a variation coefficient of 10%. To this end, a single-degree-of-freedom (SDOF) system which uses active tendon control and a three-story multiple-degree-of-freedom (MDOF) system which uses different placements of active tendons were considered. These systems have been experimentally examined by Chung et al. [28,29]. An intelligent PFLC and classic LQR controller were implemented to compare the performance of these strategies for estimating the failure probability of displacement covariance and corresponding reliability index. It was found that the PFLC performed better for reducing the structural failure of covariance responses. The advantages of the intelligent controller over the classic one have been highlighted in this paper.

2. Reliability-based probabilistic control design

In motion equations for a structure, it is possible to consider unreliability as random variable Δ. This random variable is a q-dimensional vector with mean μ_Δ, covariance σ_Δ and a joint likelihood distribution. The equations of motion for an n-DOF building can be represented in the framework of state-space as [17]:

$$\dot{z} = A(\Delta)z + B(\Delta)u + E(\Delta)w \tag{1}$$

where the measurement equation is [17]:

$$y = C(\Delta)z + D(\Delta)u + F(\Delta)v \tag{2}$$

where z is a $2n$-dimensional vector of velocity and displacement, A is a $2n\times 2n$ system plant matrix, u is an r-dimensional input vector, B is a $2n \times 2n$ matrix describing the position of the applied control forces, w is an l-dimensional vector of excitation, E is a $2n \times l$ matrix defining the effects of the excitation method on the building, y is an m-dimensional measuring vector, C is an $m \times 2n$ output matrix of the combined measured states, D is an $m\times r$ feed-through matrix, v is an m-dimensional vector for measuring noise and F is an $m \times m$ matrix that affects measurement noise.

White noise is the mathematical idealization of a stationary random process with no correlation between the values of the process at different times. Parameter $[w'v']'$ denotes a white noise vector of zero mean and autocorrelation function as [17]:

$$E\begin{bmatrix} w \\ v \end{bmatrix} = 0 \tag{3}$$

$$E\left[\begin{Bmatrix} w(t) \\ v(t) \end{Bmatrix}\left\{ w'(t+\tau) \quad v'(t+\tau) \right\}\right] = 2\pi S\delta(\tau) \tag{4}$$

where $E[\cdot]$ denotes the mathematical expectation, S denotes a matrix of uniform spectral density and δ denotes the Dirac function [17].

The principle of covariance control was developed in the 1980s [30]. The fundamental quantities, which are the product of impulsive inputs and initial conditions, are added one at a time to the structure described by Eqs. (1) and (2). These quantities are of special importance in the formulation of covariance theory. The total sum effect of all excitations applied one at a time satisfies [31]:

$$0 = X_{uwx}A^T + AX_{uwx} + BUB^T + DWD^T + X_0 \tag{5}$$

where $X_{uwx} = X + X_w + X_x$, U is the square of the matrix of input impulsive disturbance magnitudes, W is the square of the matrix of disturbance magnitudes, matrix X_w contains information about system excitation caused by impulsive perturbation $w(t)$, X contains information about system excitation due to impulsive inputs in $u(t)$ and matrix Xx contains information about the excitation of the system caused by initial condition $X0$ [31].

The formulation of covariance theory is based on these basic concepts. One reason for the development of covariance control theory is that the requirements for many engineering systems are stated in terms of the variance of state variables [31].

Failure occurs when a safe area first appears in one of the reaction values for a device model. The safe area is limited by the failure thresholds at different failure possibilities. It is often assumed that structural failure will occur when the magnitudes of the structural response exceed specified values. Failure is expected to occur in a structure when displacement covariance response σ_x exceeds allowable value σ_0.

In the context of structural reliability, the definition of a limit state is applied to better identify failure. A limit state is the boundary between the desirable and undesirable performance of a structure against failure. This boundary can also be mathematically interpreted using a limit state function [32]. When using the stationary covariance matrix response for stochastic structures, the limit state equation can be written as [17]:

$$g^i(\Delta;u) = \sigma_{0_i} - \sigma_{x_i}[\Delta;u] \tag{6}$$

where $\sigma_{x_i}[\Delta;u]$ denotes the i^{th} stationary displacement covariance response and depends on the uncertainty parameter and chosen control technique and σ_{0_i} denotes the target value [17]. The failure probability is proportional to the probability of undesirable output [32]; thus, it can be described using the limit state function as [17]:

$$P_f = P(g^i(\Delta;u) \le 0) \tag{7}$$

2.1. Reliability analysis

The current study used the MC algorithm to determine the structural reliability of a structural model. The MC simulation makes it possible to evaluate the estimation of failure probability which satisfies Eq. (8) as [33]:

$$P_f = \frac{1}{N}\sum_{i=1}^{N} I(\Delta) \tag{8}$$

where $I(\Delta)$ is defined as [33]:

$$I(\Delta) = \left\{ \begin{array}{l} 1 if g(\Delta;u) \le 0 \\ 0 if g(\Delta;u) > 0 \end{array} \right\} \tag{9}$$

and N independent sets of simulated values of Δ are generated using the probability distribution of each random variable. The likelihood of structural failure is determined using MC reliability analysis as [33]:

$$P_f = \frac{N_H}{N} \tag{10}$$

where N_H is the total number of failures.

3. Structural model

Two structural models have been used for probabilistic reliability analysis in the present study. The first is a single-degree-of-freedom (SDOF) model with active tendons, which was empirically investigated by Chung et al. [28]. The second is a three-degree-of-freedom (3DOF) single-bay building with an active tendon controller. This structure is comparable to one reported on by Chung et. al [29]. The active tendon system contains two activators, a control element and four prestressed cables. In structures with MDOF, for each degree of freedom, two activators, a controller and four additional prestressed cables are required. These structures were selected because of their wide spread popularity.

3.1. SDOF structural model

The active tendon SDOF system is shown in Fig. 1(a). In the static state, the prestress force of each tendon is denoted as R. Eqs. (11) and (12) govern the motion of uncontrolled and controlled SODF buildings, respectively, with active tendons as:

$$m\ddot{x} + c\dot{x} + kx = -m\ddot{x}_g \tag{11}$$

$$m\ddot{x} + c\dot{x} + kx = -m\ddot{x}_g - 4k_c u cos\alpha \tag{12}$$

where $\times$ is the horizontal relative displacement, u is the activator situation, c, k, and m are the damping, stiffness and mass of the building. respectively, k_c is the stiffness of the tendons and x_g is the ground acceleration. The definition of the equations of motion in state-space is:

$$\dot{z} = \begin{bmatrix} 0 & 1 \\ -\frac{k}{m} & -\frac{c}{m} \end{bmatrix} z + \begin{bmatrix} 0 \\ -\frac{4k_c cos\alpha}{m} \end{bmatrix} u + \begin{bmatrix} 0 \\ -1 \end{bmatrix} \ddot{x}_g \tag{13}$$

where $z = [x \quad \dot{x}]'$. The controller is realized by assuming that the ground acceleration can be modeled as Gaussian white noise. The SDOF model parameters are listed in Table 1.

Table 1
Model parameters of SDOF structures [17].

	Mean (μ)	Standard deviation (σ)
c (lb-s/in)	9.02	0.902
k (lb/in)	7934	793.4
m (lb-s^2/in)	16.69	1.669
k_c (lb/in)	2124	0
α (°)	36	0

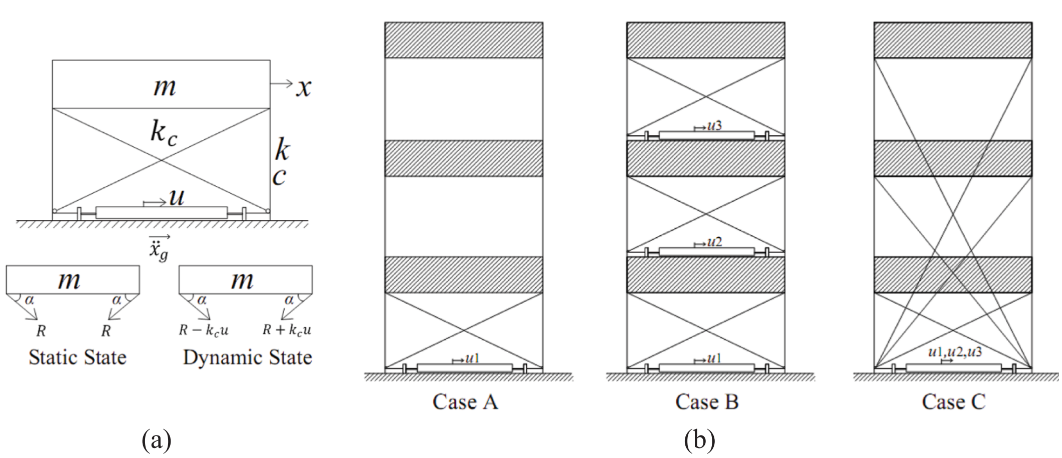

Fig. 1. Modeled structures: (a) SDOF model with active tendons [24]; (b) MDOF systems with active tendons [29].

3.2. Structural MDOF model

More complicated structures have been used as MDOF systems with different tendon controller positions. Each system is a single-bay three-story structure exposed to 1-D earthquake excitation (Fig. 1b). In case A, tendons exist only on the first floor. Cases B and C have tendons on all floors; however, all actuators are located on the ground floor in case C [34]. The mass, stiffness and damping matrices for a simple shear frame are shown in Eq. (14) and the equations of motion for controlled structures in cases A, B and C are given in state-space form in Eqs. (15), (16), and (17), respectively.

$$\kappa Q_{CL} \geq Q_{UF}[M] = \begin{bmatrix} m_1 & 0 & 0 \\ 0 & m_2 & 0 \\ 0 & 0 & m_3 \end{bmatrix}, [C] = \begin{bmatrix} c_1+c_2 & -c_2 & 0 \\ -c_2 & c_2+c_3 & -c_3 \\ 0 & -c_3 & c_3 \end{bmatrix}, [K] = \begin{bmatrix} k_1+k_2 & -k_2 & 0 \\ -k_2 & k_2+k_3 & -k_3 \\ 0 & -k_3 & k_3 \end{bmatrix} \tag{14}$$

$$[M]\ddot{X} + [C]\dot{X} + [K]X = -[M][1]\ddot{X}_g - 4K_c cos\alpha \begin{bmatrix} u_1 \\ 0 \\ 0 \end{bmatrix} \tag{15}$$

$$[M]\ddot{X} + [C]\dot{X} + [K]X = -[M][1]\ddot{X}_g + 4K_c cos\alpha \begin{bmatrix} -1 & 1 & 0 \\ 0 & -1 & 1 \\ 0 & 0 & -1 \end{bmatrix} \begin{bmatrix} u_1 \\ u_2 \\ u_3 \end{bmatrix} \tag{16}$$

$$[M]\ddot{X} + [C]\dot{X} + [K]X = -[M][1]\ddot{X}_g - 4K_c \begin{bmatrix} u_1 cos\alpha \\ u_2 cos\beta \\ u_3 cos\theta \end{bmatrix} \tag{17}$$

where c_i, k_i and m_i, respectively, are the damping, stiffness and mass of the i^{th} floor of the structure. The state of the activator is denoted as u. Eqs. (15)-(17) can be written in matrix form as:

$$M_s\ddot{x} + C_s\dot{x} + K_s x = B_s u - M_s\Gamma_s\ddot{x}_g \tag{18}$$

If the state vector is defined as $z = [x' \quad \dot{x}']'$, Eq. (1) can be rewritten in the framework of the state-space matrices as:

$$A = \begin{bmatrix} 0 & I \\ -M_s^{-1}K_s & -M_s^{-1}C_s \end{bmatrix}, [B] = \begin{bmatrix} 0 \\ M_s^{-1}B_s \end{bmatrix}, E = \begin{bmatrix} 0 \\ -\Gamma_s \end{bmatrix} \tag{19}$$

In this paper, the controller is assumed to be deterministic and the simulation parameters, damping, stiffness and mass are Gaussian random variables. A dispersion coefficient of 10% has been considered for the random variables. There is no correlation between the mass, damping and stiffness of different floors. The model parameters are defined in Table 2 as described by Chung et al. [29].

Table 2
Three-story model parameters [29].

	Mean (μ)	Standard deviation (σ)
c_1 (lb-s/in)	2.6	0.26
c_2 (lb-s/in)	6.3	0.63
c_3 (lb-s/in)	0.35	0.035
k_1 (lb/in)	5034	503.4
k_2 (lb/in)	10,965	1096.5
k_3 (lb/in)	6135	613.5
m_1 (lb-s^2/in)	5.6	0.56
m_2 (lb-s^2/in)	5.6	0.56
m_3 (lb-s^2/in)	5.6	0.56
k_c (lb/in)	2124	0
θ (°)	65	0
β (°)	55	0
α (°)	36	0

4. Control methods

4.1. LQR controller

In the LQR controller, all state variables must be measured and state feedback control must be used. The state feedback LQR controller was identified by modeling the ground acceleration as Gaussian white noise. The quadratic performance indices for the SDOF and MDOF structures are shown in Eqs. (20) and (21), respectively, as:

$$J = \lim_{T\to\infty}\frac{1}{T}E\left[\int_0^T \left(kx^2 + \gamma k_c u^2\right)dt\right] \tag{20}$$

$$J = \lim_{T\to\infty}\frac{1}{T}E\left[\int_0^T \left(x'K_s x + \gamma k_c u^2\right)dt\right] \tag{21}$$

where γ is a control scheme factor. As γ increases, more weight is given to incoming energy and, as γ decreases, more weight is put on the strain energy [29].

4.2. Probabilistic fuzzy logic controller

There are four main components of PFLS: probabilistic fuzzification, fuzzy rules, probabilistic fuzzy inference engine and probabilistic defuzzification (Fig. 2).

The rule base was developed from expert knowledge. These rules are stated in IF-THEN form as [14]:

Rule *i*: If.x_1 is $\widetilde{A}_{1,i}$ and x_2 is $\widetilde{A}_{2,i}$… and x_n is $\widetilde{A}_{n,i}$, then y is $\widetilde{B}_i$ (22).

where $\widetilde{A}_{1,i}$ ($j = 1, 2, \ldots, n$) ($i = 1, 2, \ldots, J$) is a priori for the j^{th} input variable x_j, in the i^{th} rule, and $\widetilde{B}_i$ is a subsequent section associated with output parameter y [14]. In PFLS, the antecedents and consequents are probabilistic fuzzy sets (PFSs).

4.3. Probabilistic fuzzification

The fuzzification methods of PFLS are based on the probabilistic fuzzy sets. The incorporation of primary MF and secondary PDF leads to PFS in probabilistic fuzzy theory [13]. For input variable ×, membership grade $\mu(x)$ with the secondary PDF becomes a statistical variable. The primary MF of PFSs $\widetilde{A}_{j,i}$ and $\widetilde{B}_i$ can be employed as [15]:

$$\mu(x_{j,i}) = exp\left(-\frac{\left(x_j - c_{j,i}\right)^2}{2\xi_{j,i}^2}\right) \tag{23}$$

where $\mu(x_{j,i})$ is the primary fuzzy membership grade and $\xi_{j,i}$ and $c_{j,i}$, respectively, are the width and center of the PFS. The secondary PDF is described in the primary MF by randomization of the parameters (Fig. 3).

In this study, center $c_{j,i}$ is a Gaussian distributed variable. It is feasible to write the secondary PDF as [15]:

$$p_{\tilde{A}_{j,i}}(\mu_{j,i}, x_j) = \frac{1}{2\sqrt{2\pi}\mu_{j,i}\sigma_{j,i}}\sqrt{\frac{-2\xi_{j,i}^2}{ln\mu_{j,i}}} \times \left(exp\left(-\frac{\left(\sqrt{-2\xi_{j,i}^2 ln\mu_{j,i}} + x_j - u_{j,i}\right)^2}{2\sigma_{j,i}{}^2}\right) + exp\left(-\frac{\left(-\sqrt{-2\xi_{j,i}^2 ln\mu_{j,i}} + x_j - u_{j,i}\right)^2}{2\sigma_{j,i}{}^2}\right)\right) \tag{24}$$

where $\mu_{j,i} \in [0, 1]$ is the primary fuzzy degree parameter, $p_{\tilde{A}_{j,i}}(\mu_{j,i}, x_j)$ is the probability density function and $\sigma_{j,i}$ and $u_{j,i}$, respectively, are the standard deviation and mean of the Gaussian distribution in terms of $c_{j,i}$.

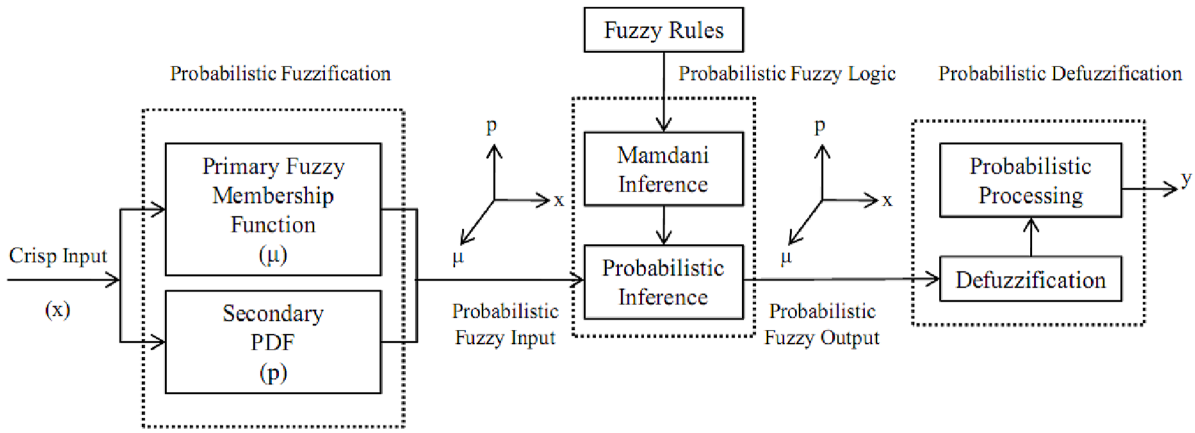

Fig. 2. Structure of PFLS [14].

4.4. Probabilistic fuzzy inference engine

As PFS consists of a continuous probability density function, the inference engine of PFLS can be obtained using a probabilistic framework. Nonlinear mapping between input domain $X_1 \times X_2 \times \cdots \times X_n$ and output domain Y can be represented using the probabilistic fuzzy inference engine as [14,15]:

$$R_{\tilde{A}_{1,i}\times\cdots\times\tilde{A}_{n,i}\rightarrow\tilde{B}_i}(x,y) \tag{25}$$

Fuzzy relationship set R_i in Y can be determined using Eq. (26) for input $\times = (x_1,\ldots,x_n)$ and the associated MF$\mu_X(x)$ as [15]:

$$\mu_{R_i}(y) = \mu_{A_{1,i}}{}^{\circ}\mu_{A_{2,i}}{}^{\circ}\cdots{}^{\circ}\mu_{A_{M,i}}{}^{\circ}\mu_{B_i} \tag{26}$$

where $\mu_{A_{j,i}}$ and μ_{B_i} describe the fuzzy membership grade. Symbol "o" denotes a t-norm operation [15]. In this study, minimum operation has been used. The probabilistic fuzzy inference in the i^{th} rule is [15]:

$$\mu_{R_i}(y)\ p_{R_i} = p(\overset{j=1}{\underset{n}{T}}\mu_{A_{j,i}}(y_i)^{*}\mu_{B_i}(y)) = p(min(\mu_{A_{1,i}}(x_1),\cdots,\mu_{A_{M,i}}(x_M))^{*}\mu_{B_i}(y)) \tag{27}$$

where p_{R_i} is the probability density function of $\mu_{R_i}(y)$ and T, and * denotes the minimum functioning [15]. The PDF of the input firing level can be written as [14,15]:

$$\begin{aligned} p\left(\mu_{A_i}(x)\right) &= p\left(\overset{n}{\underset{j=1}{T}}\mu_{\tilde{A}_{j,i}}(x_j)\right) = p\left(\min\left(\mu_{\tilde{A}_{j,i}}(x_1),\ldots,\mu_{\tilde{A}_{j,i}}(x_n)\right)\right) \\ &= \sum_{t}^{n-1} p\left(\mu_{\tilde{A}_{i,j}}(x_t)\right)\prod_{j=t+1}^{n}\left(1-p\left(\mu_{\tilde{A}_{i,j}}(x_j)\right)\right) + \sum_{t=1}^{n-1} p\left(\mu_{\tilde{A}_{i,j}}(x_t)\right)\left[-\sum_{k=t+1}^{n} p\left(\mu_{\tilde{A}_{i,j}}(x_t)\right)\times\prod_{j=t+1}^{n}\left(1-p\left(\mu_{\tilde{A}_{i,j}}(x_j)\right)\right)\right] \\ &\quad + p\left(\mu_{\tilde{A}_{i,j}}(x_n)\right) \end{aligned} \tag{28}$$

where $\mu_{A^i}(x)$ is the firing level of the input variable in the i^{th} rule and $P(\mu_{\tilde{A}_{j,i}}(x_j))$ is the cumulative distribution function (CDF) of $\mu_{\tilde{A}_{j,i}}$. The PDF of inference PFS $p(\mu_{R_i}(y))$ can be presented as [14,15]:

$$\begin{aligned} p(\mu_{R_i}(y)) &= p(min(\mu_{A^i}(x),\mu_{\tilde{B}_i}(y))) \\ &= p(\mu_{A^i}(x))(1-P(\mu_{\tilde{B}_i}(y))) - P(\mu_{A^i}(x))p(\mu_{\tilde{B}_i}(y)) + p(\mu_{\tilde{B}_i}(y)) \end{aligned} \tag{29}$$

where $P(\mu_{\tilde{B}_i}(y))$ and $P(\mu_{A^i}(x))$ are the CDF of $\mu_{\tilde{B}_i}(y)$ and $\mu_{A^i}(x)$, respectively.

4.5. Probabilistic defuzzification

The defuzzification technique is related to the fuzzy sets. As the inference engine is based on probabilistic fuzzy sets, the defuzzification method is associated with probability. Thus, a probabilistic defuzzification is proposed herein. The probabilistic defuzzification produces the final crisp output y based on the mathematical expectation of probabilistic output y_{PFLS} as [15]:

$$y = E(y_{PFLS}) = \sum y_{PFLS}\cdot P(y_{PFLS}) \tag{30}$$

where $P(y_{PFLS})$ is the probability of y_{PFLS}. The probabilistic output of the probabilistic fuzzy logic system can be calculated based on the center-of-the set probabilistic defuzzification method as [14]:

$$y_{PFLS} = \frac{\sum_{i=1}^{J} y_i\mu_{A^i}}{\sum_{i=1}^{J}\mu_{A^i}} \tag{31}$$

where y_i is the center of probabilistic fuzzy set $\widetilde{B}_i$ in rule i, J is the number of rules and μ_{A^i} is the firing level in rule i.

One limitation of probabilistic theory is the challenge of obtaining the likelihood distribution of the product of parameters y_i and μ_{A^i}. To overcome this inadequacy, it is proposed to replace y_i with the mathematical expectation of y_i as shown in Eq. (32) [15]. The discretization method is then required to obtain y_{PFLS} using Eq. (33) [15]. In this process, firing level μ_A^i ($p(\mu_A^i) > 0$) should be discretized into Q regions $[\underline{\mu_{A^{i,t_i}}}, \overline{\mu_{A^{i,t_i}}}]$ which are centered at $\mu_{A^{i,1}}, \mu_{A^{i,2}}, \ldots, \mu_{A^{i,Q}}$'; thus, associated probability $P(\mu_{A^{i,1}}), P(\mu_{A^{i,2}}), \ldots, P(\mu_{A^{i,Q}})$ can be estimated using Eq. (34) [15].

$$y_{PFLS} = \frac{\sum_{i=1}^{J} E(y_i)\mu_{A^i}}{\sum_{i=1}^{J}\mu_{A^i}} \tag{32}$$

$$y_{PFLS} = \left\{\frac{\sum_{i=1}^{J} E(y_i)\mu_{A^{i,t_i}}}{\sum_{i=1}^{J}\mu_{A^{i,t_i}}}\right\}, t_i \in \{1,\ldots,Q\} \tag{33}$$

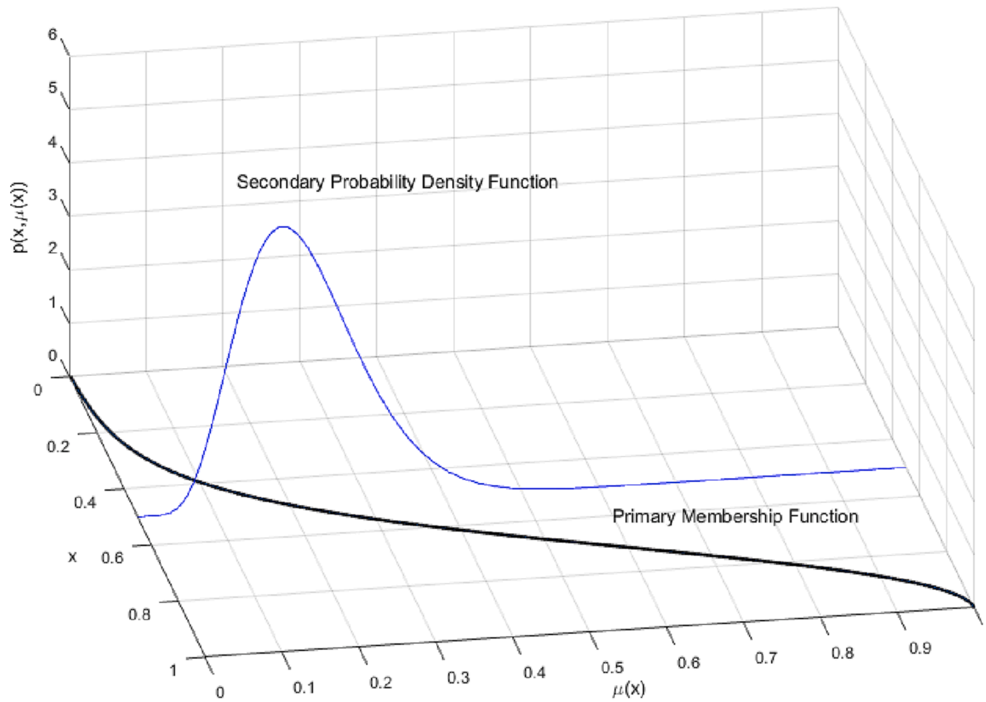

Fig. 3. Probabilistic fuzzy set.

$$P(\mu_{A^{i,t_i}}) = \int_{\underline{\mu_{A^{i,t_i}}}}^{\overline{\mu_{A^{i,t_i}}}} p(\mu_{A^i}) d(\mu_{A^i}) \tag{34}$$

Every possible combination of $\{\mu_{A^{1,t_1}}, \mu_{A^{2,t_2}}, \ldots, \mu_{A^{J,t_J}}\}$ $(t_i = 1, \cdots, Q, i = 1, \cdots, J)$ and the associated probabilities should be considered in order to detect both y_{PFLS} and the related $P(y_{PFLS})$ as [15]:

$$p(y_{PFLS}) = \prod_{i=1}^{J} p(\mu_{A^{i,t_i}}) \tag{35}$$

4.6. Probabilistic fuzzy logic scheme

A probabilistic fuzzy logic controller uses uncertain data received directly from the structure. In this study, PFLC applies the displacement and velocity of the structure as input variables, each with three primary MFs and the active control force as an output variable with seven primary MFs. Two input variables are used to define the fuzzy space and describe the efficiency of the PFLS strategy for the control problem.

Gaussian functions are expressed as the specified mean and standard deviation. Thus, Gaussian functions describe uncertainty more accurately than other functions (e.g. triangular, trapezoidal, z-shaped and s-shaped functions). Therefore, the Gaussian primary MF for the input and output variables can be implemented as described in Eq. (23) using the common interval of [-1, 1].

PFLC is used here as a stochastic active controller. The membership function is thus transformed from a simple mathematical model to a probability parameter. Integrating the Gaussian and probability within the membership function is believed to give a better answer. Here, PFS has been constructed by randomly selecting the center of the Gaussian fuzzy set; thus, MF becomes a random parameter that can be introduced by the secondary PDF function. As presented in Eq. (24), the standard deviation and mean of the fuzzy sets are secondary PDF features of each primary MF.

Fig. 4(a) and 4(b) depict the suggested primary MFs for the input and output variables. For both the inputs and output, the same standard deviation is assumed for the center of the fuzzy sets. The mean centers of the primary MFs are −1, 0, 1 for the input variables and −0.75, −0.5, −0.25, 0, 0.25, 0.5, 0.75 for the output variable. Table 3 shows the fuzzy variables [10] and the inference rule is presented in Table 4.

5. Results and discussion

Two control strategies have been considered when studying the efficiency of controlled structures in reliability analysis: the classic LQR controller and intelligent PFLC. The mass, stiffness and damping variables used for SDOF and MDOF structures were random Gaussian variables with a 10% dispersion coefficient. The structures were exposed to dynamic random loading modeled as Gaussian white noise. MC reliability analysis was used to assess the reliability of the controlled structures. In the design of the LQR controller, a full-state feedback closed-loop system has been used. Control design parameter $\gamma = 1$ was chosen as the performance index for the LQR controller (Eqs. (20) and (21)).

Spencer et al. [17] showed that the selection of a smaller γ value allows more weight to be placed on the strain energy, which will obtain a smaller covariance matrix (RMS) response for displacement. In optimal control theory, the focus is on finding the control gain matrix which can be solved using the Riccati algorithm. Table 5 presents the gain matrices of the SDOF and MDOF systems. Table 6 lists the nominal covariance responses of displacement and velocity (σ_x and σ_x) for the top floor of the SDOF and MDOF structures exposed to unit intensity white noise.

The results in Table 6 for the SDOF model indicate that PFLC reduced the covariance responses of the displacement and velocity of the top floor by 38.6% and 50.6%, respectively, compared to the LQR controller. Moreover, as compared to the LQR controller, PFLC reduced the displacement covariance response. These results for the top floor in cases A, B and C were 12.5%, 36.1% and 20%, respectively (Table 6), and the corresponding results for the velocity response were 17.6%, 9.83% and 15.2%, respectively. The simulation results for the SDOF and MDOF structures show that PFLC was able to reduce the RMS responses of the top floor.

Fig. 5(a) and 5(b) show the failure probability results of the controlled displacement covariance responses of the SDOF structure and MDOF structures using the LQR controller and PFLC for different

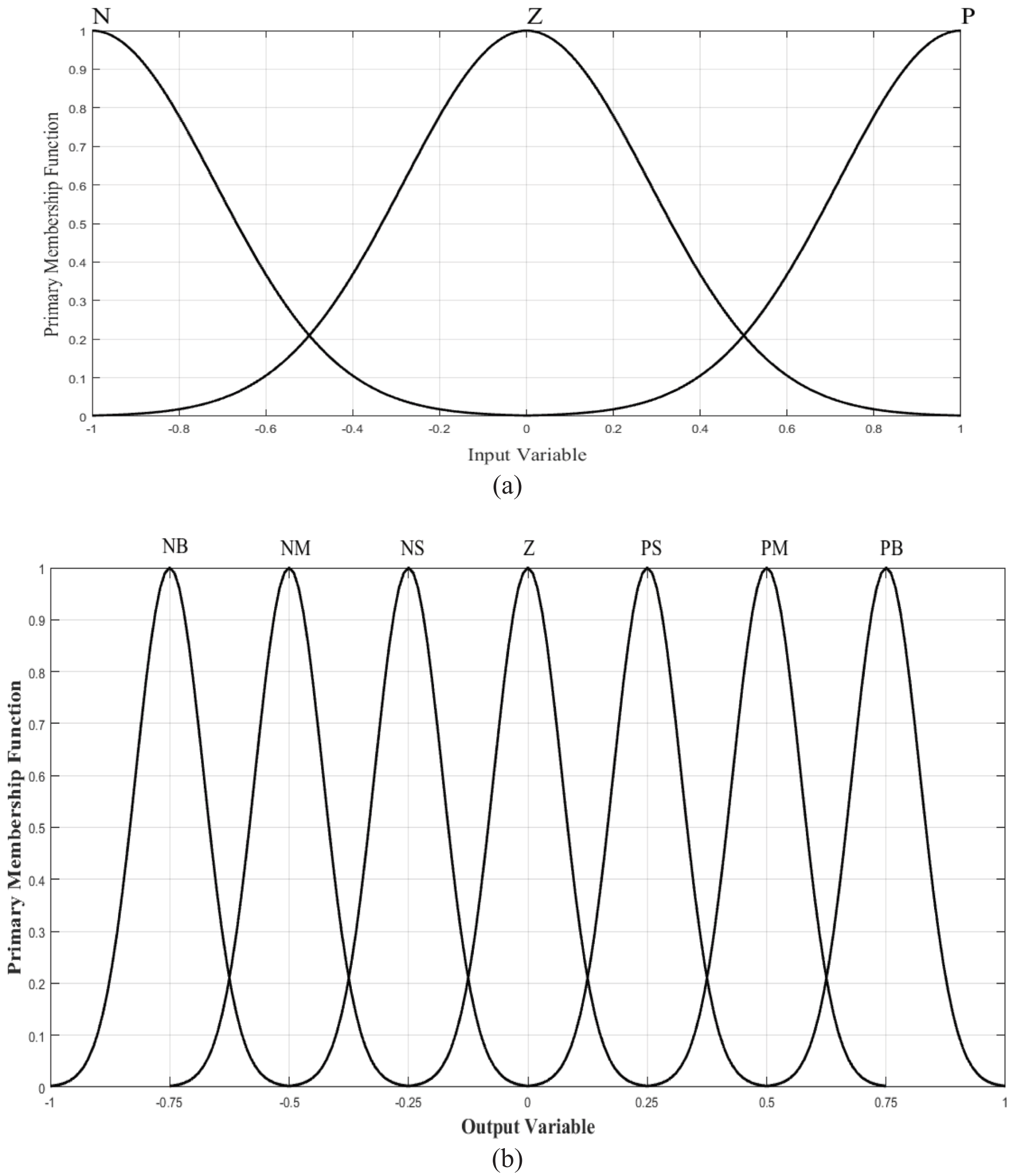

Fig. 4. Membership functions: (a) primary MFs of input variables; (b) primary MFs of output variables.

threshold levels of σ_0. As shown in Fig. 5(a), MC reliability analysis of the SDOF structure determined failure probabilities of up to 10^{-5} for both the PFLC and LQR controllers. However, the results indicate that the PFLC resulted in the smallest failure probability compared to the LQR controller because of the higher threshold level. As shown in Table 7 for the SDOF structure, the likelihood of a displacement covariance response being greater than 0.0126 in were 9.90e-1 and 2.00e-5, respectively, for the LQR controller and PFLC. This indicates a significant reduction in the failure probability.

As shown in Fig. 5(b) for case A, the use of the LQR controller and PFLC caused a slight variation (in the failure probability) at large failure probabilities. It can be seen that the MC reliability analysis measured the failure probabilities of up to 10^{-4} and 10^{-5} for increasing threshold levels for the LQR controller and PFLC, respectively (Fig. 5(b)). The occurrence of failure decreased with the use of the intelligent PFLC, which increased the reliability index. The robustness of the controlled-response efficiency in case A for both PFLC and the LQR controller as obtained by MC reliability analysis is shown in Table 7. The limit state probabilities of an MC displacement response greater than 0.077 in were 2.52e-1 and 1.00e-5, respectively, for the LQR controller and PFLC. However, the reliability indices for the LQR controller and PFLC were 1.9558 and 4.2650, respectively.

Table 3
Fuzzy variables.

MF	Variable	Definition
Input	*P*	positive
	Z	zero
	N	negative
Output	*PB*	positive big
	PM	positive medium
	PS	positive small
	Z	zero
	NS	negative small
	NM	negative medium
	NB	negative big

Table 4
Inference rules for PFLS.

Displacement	Velocity *N*	*Z*	*P*
N	*PB*	*PM*	*PS*
Z	*PS*	*Z*	*NS*
P	*NS*	*NM*	*NB*

Table 5
Transfer function for controllers with SDOF and MDOF.

	Control gain matrix (*G*)					
SDOF	−1.0969			−0.0717		
Case A	−2.6315	1.6872	−0.0281	−0.0646	−0.0273	−0.0099
Case B	−1.1264	0.1119	0.0453	−0.0365	−0.0158	−0.0132
	1.0777	−1.1220	−0.0533	0.0207	−0.0308	−0.0137
	−0.1181	1.1065	−1.-258	0.0026	0.0197	−0.0363
Case C	−1.3385	0.4691	0.1108	−0.0453	0.0021	0.0028
	−0.1124	−0.8408	0.3168	0.0015	−0.0425	0.0033
	0.0585	−0.0819	−0.5044	0.0015	0.0024	−0.0393

Table 6
Nominal RMS displacement and velocity for top floor of SDOF and MDOF structures using LQR controller and PFLC.

	Nominal covariance responses					
	σ_x (in)			$\sigma_{\dot{x}}$(in/s)		
	No control	LQR controller	PFLC	No control	LQR controller	PFLC
SDOF	0.1688	0.0162	0.0099	3.6862	0.4940	0.2442
Case A	0.6648	0.0624	0.0546	9.9477	1.1646	0.9598
Case B	0.6133	0.0310	0.0198	9.4697	0.6576	0.5929
Case C	0.6582	0.0236	0.0189	9.9450	0.5766	0.4887

In case B, with tendons on all floors, MC reliability analysis showed that PFLC led to a lower failure probability than the LQR controller for threshold levels of $\sigma_0 < 0.0345$ in (Fig. 5(b)). Further, the results for $\sigma_0 > 0.0345$ in indicate that PFLC led to a greater failure probability than the LQR controller for large responses. The failure probability for $\sigma_0 = 0.0345$ in was about 7.75e-2 for both PFLC and the LQR controller. However, the failure probability decreases smoothly for PFLC compared to the LQR controller (Fig. 5(b)).

Fig. 5(b) shows that MC reliability analysis for the LQR controller provided a failure probability of up to 2.00e-5 for a threshold level of $\sigma_0 = 0.042$ in and that an increase in the threshold level to 0.20 in in the PFLC led to a failure probability of about 6.00e-5. For example, Table 7 presents the probability of exceedance of a specified displacement threshold level which is less than 0.0345 in for case B. As shown, PFLC produced a failure probability of about 8.00e-2 at a threshold level of $\sigma_0 = 0.033$ in, while the corresponding value for the LQR controller was about 1.119e-1. The reliability values at a threshold level of $\sigma_0 = 0.033$ in were 1.30 and 1.20, respectively, for PFLC and the LQR controller.

As shown in Fig. 5(b) for case C, MC reliability analysis determined the failure probability up to 10^{-5} for both PFLC and the LQR controller as the threshold level increased. The controlled structure in case C using PFLC caused a decrease in the failure probability compared to the LQR controller for a threshold level of $\sigma_0 < 0.0325$ in. The results also showed that, at a threshold level of $\sigma_0 = 0.0325$ in, the failure probability was about 5.20e-4. Finally, PFLC increased the failure probability for a threshold level of $\sigma_0 > 0.0325$ in compared to the LQR controller. For example, Table 7 shows the probability of exceedance of a specified displacement threshold level of $\sigma_0 < 0.0325$ in for case C. As shown, PFLC produced a failure probability of about 2.92e-2 at a threshold level of $\sigma_0 = 0.025$ in, while the corresponding value for the LQR controller was about 3.03e-1. The reliability values at a threshold level of $\sigma_0 = 0.025$ in were 1.89 and 0.52, respectively, for PFLC and the LQR controller.

Fig. 6(a) and 6(b) show the CDF for the controlled displacement covariance response of the SDOF and MDOF structures. The use of PFLC for the SDOF structure reduced the controlled displacement response compared to use of the LQR controller (Fig. 6(a)).

Fig. 6(b) shows the CDF for cases A, B, and C for both PFLC and the LQR controller to compare to the efficiency of the traditional LQR controller and intelligent PFLC on the failure probability of controlled displacement responses for MDOF structures. In case A, the PFLC caused a substantial decrease in the roof level displacement covariance response compared to the LQR controller. A greater probability of large responses in the displacement covariance resulted from the use of the LQR controller compared to PFLC. The corresponding nominal response for PFLC on the top floor in case A was about 12.5% less compared to the classic LQR controller (Table 6).

Fig. 6(b) shows that the CDF for the controlled structure in case B with PFLC was a wide distribution function. However, the corresponding results for the LQR controller show a narrow function for the same samples. Also, in case C, PFLC significantly decreased the displacement covariance response of the roof level compared to the LQR controller.

When comparing the safety of the controlled buildings with PFLC, case A had the most responses for the same failure probability compared to cases B and C. Considering a failure likelihood of 0.20 (20%) as the threshold level, Fig. 6(b) shows that the corresponding controlled covariance responses were about 0.0512, 0.0113 and 0.0169 in for cases A, B and C, respectively. Moreover, the failure probability of the displacement covariance response at $\sigma_x = 0.018$ in was about 48% for PFLC in cases B and C. Note that, for displacement covariance responses of less than 0.0181 in, the failure probability in case C was larger than for case B using PFLC. However, the failure probability decreased in case C in comparison with case B for $\sigma_x > 0.0181$ in.

PFLC as a probabilistic active controller reduced the displacement covariance response and the corresponding failure probability more effectively than did the LQR controller. The results of MC reliability analysis show that the placement of active tendons on the first floor in both the PFLC and LQR controllers was sufficient. However, the use of active tendons on all floors was insufficient for reducing the failure probability and displacement responses. In case B, the LQR controller actually produced a much smaller failure probability than the PFLC for all relatively large threshold levels of displacement. The active tendons on the top floors in case B had the side effect of them experiencing reaction forces in the direction opposite to the principle control forces.

In case C, the reaction forces were supported by the ground, so the top floor RMS displacement response was smaller than that in case B (using the LQR controller). However, PFLC was able to reduce the displacement covariance responses in case B for a failure probability of less than 50% compared to case C. By contrast, for failure probabilities greater than 50%, the displacement covariance response increased compared to case C. It can be concluded that the ability of the PFLC approach to handling stochastic uncertainty in fuzzy rules reduced both

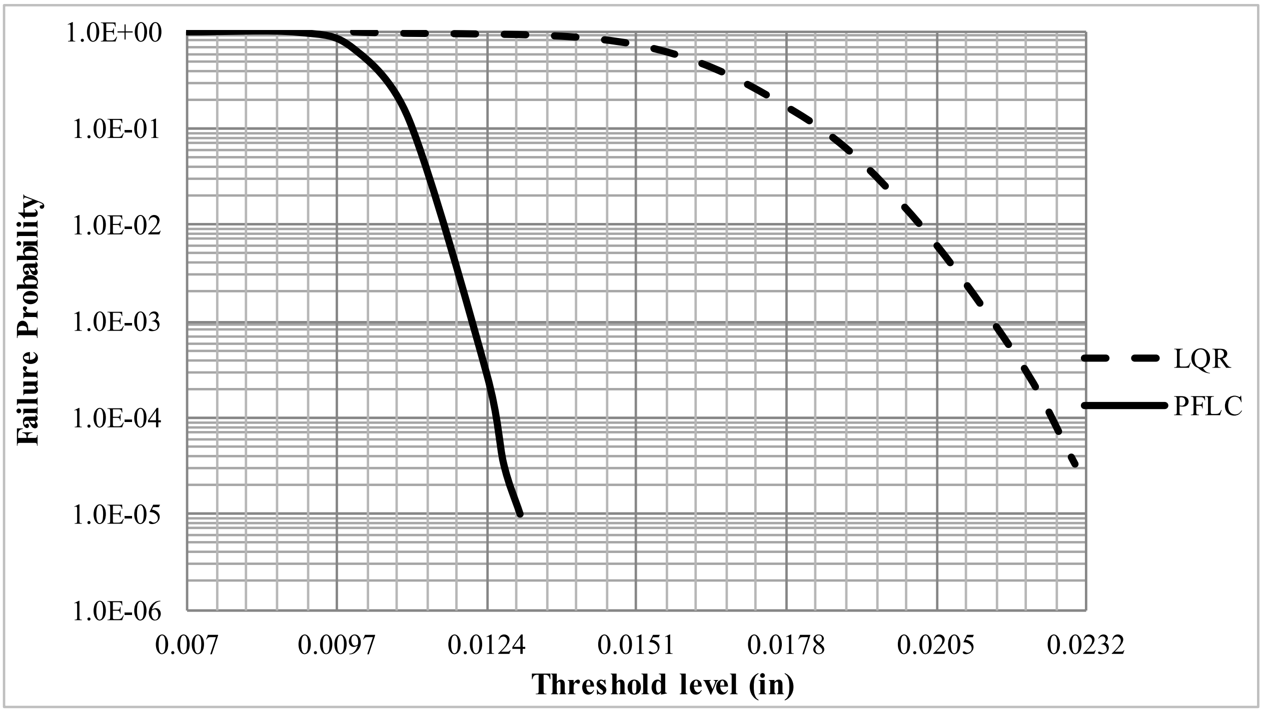

(a)

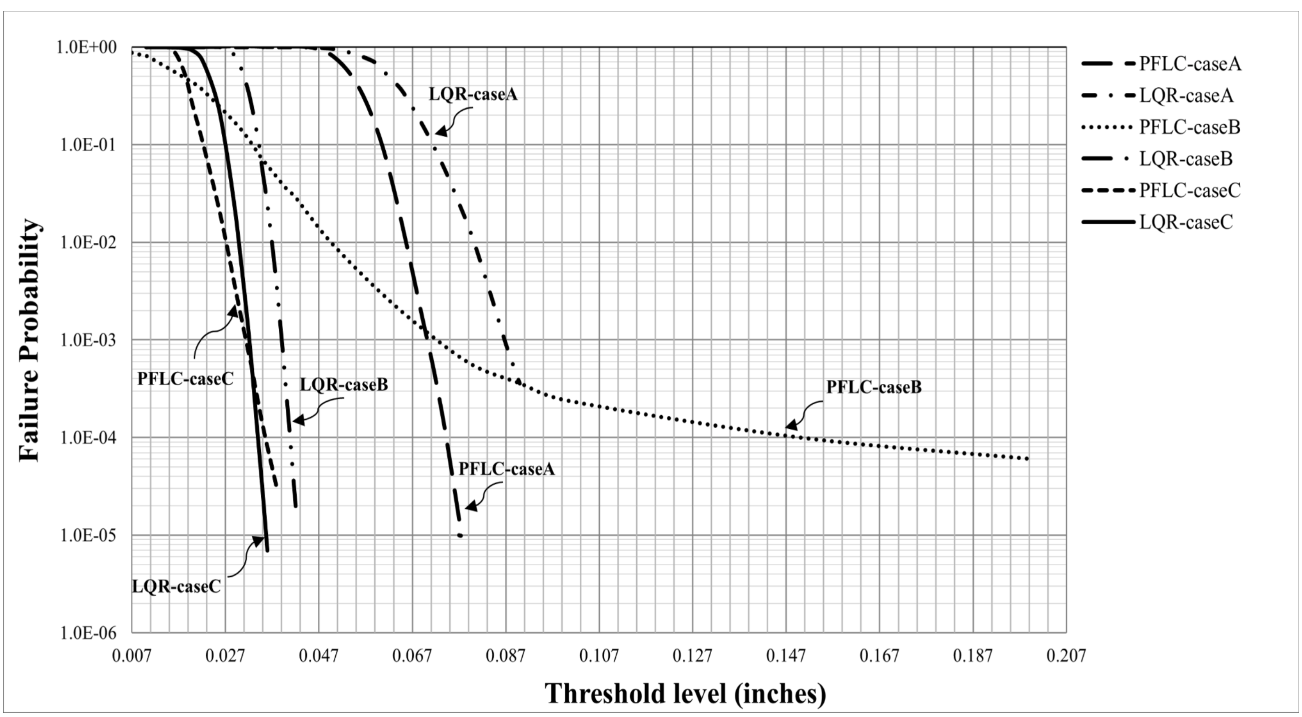

(b)

Fig. 5. Failure probability for PFLC and LQR controller using MC reliability analysis: (a) SDOF structure; (b) cases A, B and C.

the structural responses and failure probability and, subsequently, increased the reliability index. It is important to note that the reported results relate to the specific case analyzed and that a wider range of analyses seems necessary.

6. Conclusion

This study investigated the efficiency of probabilistic active control using a probabilistic fuzzy logic system for MC reliability analysis of civil engineering structures with uncertain characteristics subject to a dynamic random load which was modeled by Gaussian white noise. The

Table 7
Reliability assessment results of LQR controller and PFLC for SDOF and MDOF structures.

	SDOF P ($\sigma_x \geq 0.0126$)	Reliability index, β	Case A P ($\sigma_x \geq 0.077$)	Reliability index, β	Case B P ($\sigma_x \geq 0.033$)	Reliability index, β	Case C P ($\sigma_x \geq 0.025$)	Reliability index, β
LQR	9.90e-1	0	2.52e-1	1.9558	1.119e-1	1.20	3.03e-1	0.52
PFLC	2.00e-5	4.1075	1.00e-5	4.2650	8.00e-2	1.30	2.92e-2	1.89

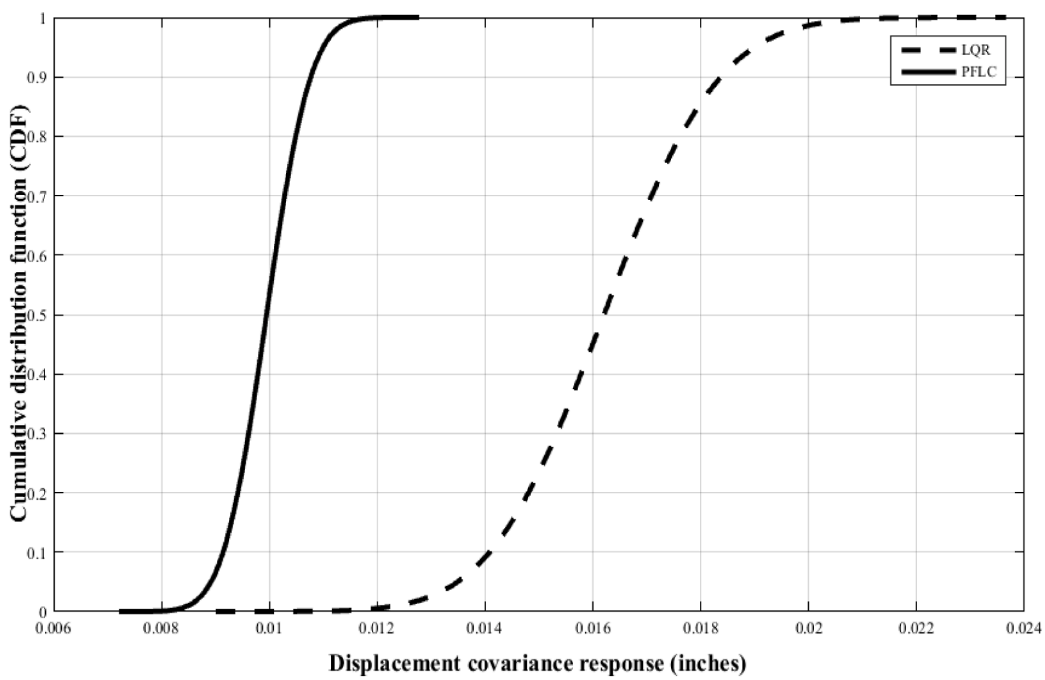

(a)

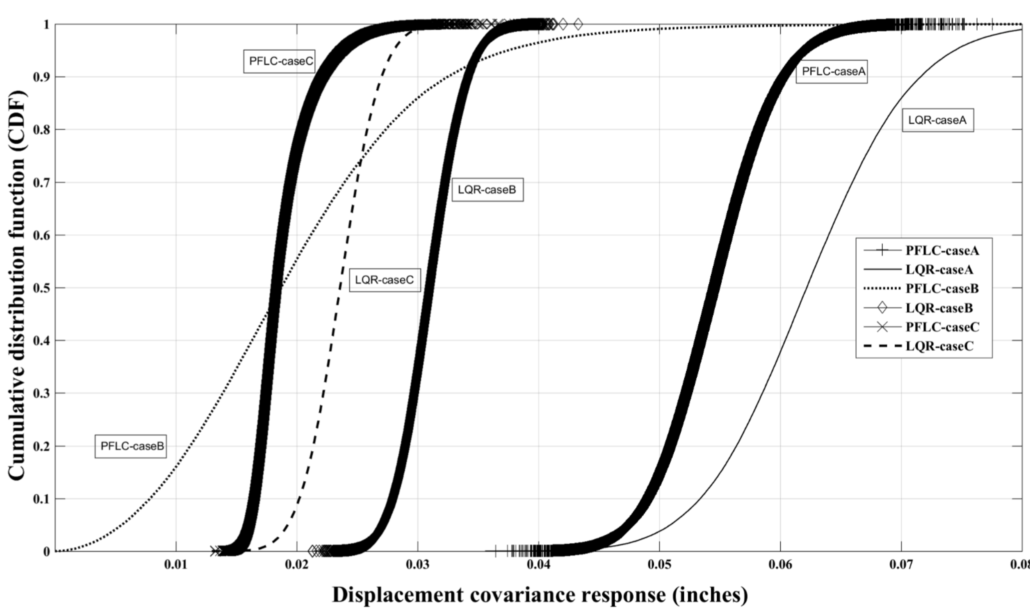

(b)

Fig. 6. CDF of controlled displacement covariance response for PFLC and LQR controllers: (a) SDOF structure; (b) cases A, B and C.

mass, stiffness and damping variables of the structures were considered to be random Gaussian parameters. The dispersion coefficient of these parameters was assumed to be 10%.

The active tendon system was investigated using structural models with a SDOF system and with a three-story MDOF system. The intelligent PFLC and classic LQR controller were implemented and their performances were compared for estimating the failure probability of displacement covariance and the corresponding reliability index of the structures. The CDF of the SDOF structure indicated that PFLC reduced the controlled displacement covariance response compared to the LQR controller. Thus, the MC reliability analysis of the SDOF structure showed that PFLC provided a lower failure probability for the same displacement response compared to the LQR controller.

The PFLC was able to estimate the failure probability up to 10^{-5} in MDOF structures as the threshold levels increased. The failure probability of the displacement covariance responses of the top floors in cases A, B and C indicated that PFLC is more accurate than the LQR controller in terms of the lower probability of an extreme displacement covariance response. Reliability analysis in case B, with tendons on all floors, showed that PFLC produced the smallest displacement for a failure probability of less than 48% compared to case C. However, reliability analysis in case C performed better for failure probabilities of greater than 48%. Since PFLC is a combination of linguistic and stochastic uncertainties, the results for the PFLC are more accurate and reliable than the LQR controller.

It is important to note that these results were obtained by assuming earthquake excitation as Gaussian white noise. It is strongly recommended that this research be continued on the benchmark structures using far-field and near-field earthquake excitation.

Funding

The authors declare no specific funding for this work.

Declaration of Competing Interest

The authors declare that they have no known competing financial interests or personal relationships that could have appeared to influence the work reported in this paper.

Acknowledgments

This research did not receive any specific grant from funding agencies in the public, commercial or not-for-profit sectors.

References

[1] Karnik NN, Mendel JM. Introduction to type-2 fuzzy logic systems. IEEE Int Conf Fuzzy Syst Proc, 2: 915-920. Anchorage, AK, USA; 1998a.
[2] Karnik NN, Mendel JM. Type-2 fuzzy logic systems: type-reduction. IEEE Int Conf Syst 2:2046-205. San Diego, CA; 1998b.
[3] Karnik NN, Mendel JM, Liang Q. Type-2 Fuzzy Logic Systems. IEEE Trans Fuzzy Syst 1999;7(6):643–58.
[4] Liang Q, Mendel JM. Interval Type-2 Fuzzy Logic Systems: Theory and Design. IEEE Trans Fuzzy Syst 2000;8(5):535–50.
[5] Karnik NN, Mendel JM. Centroid of a type-2 Fuzzy Set. Inf Sci 2001;132(1–4): 195–220.
[6] Mendel JM, John RIB. Type-2 Fuzzy Sets Made Simple. IEEE Trans Fuzzy Syst 2002;10(2):117–27.
[7] Mendel JM, John RIB, Liu F. Interval Type-2 Fuzzy Logic Systems Made Simple. IEEE Trans Fuzzy Syst 2006;14(6):808–21.
[8] Mendel JM. Advances in Type-2 Fuzzy Sets and Systems. Inf Sci 2007;177(1): 84–110.
[9] Golnargesi S, Shariatmadar H, Razavi HM. Seismic Control of Buildings with Active Tuned Mass Damper through Interval Type-2 Fuzzy Logic Controller Including Soil-Structure Interaction. Asian J Civ Eng 2018;19(2):177–88.
[10] Shariatmadar H, Golnargesi S, Akbarzadeh-T M.R. Vibration Control of Buildings Using ATMD against Earthquake Excitations through Interval Type-2 Fuzzy Logic Controller. Asian J Civ Eng (Bhrc).15 (3): 321-338; 2014.
[11] Meghdadi AH, Akbarzadeh-T MR. Probabilistic Fuzzy Logic and Probabilistic Fuzzy Systems. 10th IEEE Int. Conf. on Fuzzy Syst. 2: 1127–1130. Melbourne, VIC, Australia; 2001.
[12] Li HX, Liu Z. A Probabilistic Fuzzy Logic System: Learning in the Stochastic Environment with Incomplete Dynamics. IEEE Int. Conf. on Syst., 383-388. San Antonio, TX; 2009.
[13] Liu Z, Li HX. Probabilistic Fuzzy Logic System: a Tool to Process Stochastic and Imprecise Information. IEEE Int. Conf. on Fuzzy Syst. 848-853. Jeju Island; 2009.
[14] Zhang G, Li HX. An Efficient Configuration for Probabilistic Fuzzy Logic System. IEEE Trans Fuzzy Syst 2012;20(5):898–909.
[15] Zhang G, Li HX, Gan M. Design a Wind Speed Prediction Model Using Probabilistic Fuzzy System. IEEE Trans Industr Inform 2012;8(4):819–27.
[16] Spencer Jr BF, Kaspari DC, Sain MK. Structural control design: a reliability-based approach. Proceedings of 1994 American Control Conf. – ACC'94. 1: 1062-1066. Baltimore, MD, USA; 1994a.
[17] Spencer Jr BF, Sain MK, Won CH, Kaspari DC, Sain PM. Reliability- Based measures of Structural Control Robustness. Struct Saf 1994;15(1–2):111–29.
[18] Battaini M, Casciati F, Faravelli L. Reliability Analysis of Controlled Structures. Proceedings Intell. Inf. Syst. IIS'97, 589-593. Grand Bahama Island; 1997.
[19] May BS, Beck JL. Probabilistic Control for the Active Mass Driver Benchmark Structural Models. Earthq Eng Struct Dyn 1998;27(11):1331–46.
[20] Venini P, Mariani C. Reliability as a measure of Active Control Effectiveness. Comput Struct 1999;73(1–5):465–73.
[21] Field Jr RV, Bergman LA. Reliability-based approach to linear covariance control design. J Eng Mech 1998;124(2):193–8.
[22] Shariatmadar H, Behnam-R G. Active Control of Structures and Reliability Analysis by Subset Simulation Method. NationalPark-Forschung in Der SCHWEIZ (Switzerland Research Park Journal) 2013;102(3).
[23] Wang L, Wang X, Li Y, Lin G, Qiu Z. Structural time-dependent Reliability Assessment of the Vibration Active Control System with unknown-but-bounded Uncertainties. Struct Control Health Monit 2017;24(10):e1965.
[24] Zhang L, Zhang J, You L, Zhou S. Reliability Analysis of Structures Based on a Probability-Uncertainty Hybrid Model. Qual Reliab Eng Int 2019;35(1):263–79.
[25] Wang L, Liu J, Zhou Z, Li Y. A Two-Stage Dimension-Reduced Dynamic Reliability Evaluation (TD-DRE) Method for Vibration Control Structures Based on Interval Collocation and Narrow Bounds Theories. ISA Trans 2022.
[26] Wang L, Zhou Z, Liu J. Interval-Based Optimal Trajectory Tracking Control Method for Manipulators with Clearance Considering Time-Dependent Reliability Constraints. Aerosp Sci Technol 2022;128:107745.
[27] Liu J, Wang L. Two-Stage Vibration-Suppression framework for Optimal Robust Placements Design and Reliable PID Gains Design via Set-Crossing Theory and Artificial Neural Network. Reliab Eng Syst Saf 2023;230:108956.
[28] Chung LL, Reinhorn AM, Soong TT. Experiments on Active Control of Seismic Structures. J Eng Mech 1988;114(2):241–56.
[29] Chung LL, Lin RC, Soong TT, Reinhorn AM. Experimental Study of Active Control for MDOF Seismic Structures. J Eng Mech 1989;115(8):1609–27.
[30] Hotz A, Skelton RE. Covariance Control Theory. Int J Control 1987;46(1):13–32.
[31] Robinson, W. A Pneumatic Semi-Active Control Methodology for Vibration Control of Air Spring Based Suspension Systems. Graduate Theses and Dissertations, Iowa State University; 2012.
[32] Nowak AS, Collins KR. Reliability of Structures. Boston: McGraw-Hill; 2000.
[33] Tee KF, Khan LR, Chen H-P. Probabilistic Failure Analysis of Underground Flexible Pipes. Struct Eng Mech 2013;47(2):167–83.
[34] Nigdeli SM, Boduroglu MH. Active tendons for seismic control of buildings. Int J Civil Environ Eng 2010;4(8):267–73.